Published in final edited form as:
Adv Exp Med Biol. 2013 ; 991: 85–104. doi:10.1007/978-94-007-6331-9_6.

$PI(4,5)P_2$-Mediated Cell Signaling: Emerging Principles and PTEN as a Paradigm for Regulatory Mechanism

Arne Gericke[1], **Nicholas R. Leslie**[2], **Mathias Lösche**[3,4,5], and **Alonzo H. Ross**[6,7]

[1]Department of Chemistry and Biochemistry, Worcester Polytechnic Institute, Worcester, MA 01609 USA

[2]Division of Molecular Physiology, University of Dundee, Dundee, United Kingdom DD1 5EH

[3]Department of Physics, Carnegie Mellon University, Pittsburgh, PA 15213 USA

[4]Department of Biomedical Engineering, Carnegie Mellon University, Pittsburgh, PA 15213 USA

[5]The National Institute of Standards and Technology, Center for Neutron Research, Gaithersburg, MD 20899 USA

[6]Department of Biochemistry and Molecular Pharmacology, University of Massachusetts Medical School, Worcester, MA 01605 USA

Abstract

$PI(4,5)P_2$ (phosphatidylinositol 4,5-bisphosphate) is a relatively common anionic lipid that regulates cellular functions by multiple mechanisms. Hydrolysis of $PI(4,5)P_2$ by phospholipase C yields inositol trisphosphate and diacylglycerol. Phosphorylation by phosphoinositide 3-kinase yields $PI(3,4,5)P_3$, which is a potent signal for survival and proliferation. Also, $PI(4,5)P_2$ can bind directly to integral and peripheral membrane proteins. As an example of regulation by $PI(4,5)P_2$, we discuss phosphatase and tensin homologue deleted on chromosome 10 (PTEN) in detail. PTEN is an important tumor suppressor and hydrolyzes $PI(3,4,5)P_3$. $PI(4,5)P_2$ enhances PTEN association with the plasma membrane and activates its phosphatase activity. This is a critical regulatory mechanism, but a detailed description of this process from a structural point of view is lacking. The disordered lipid bilayer environment hinders structural determinations of membrane-bound PTEN. A new method to analyze membrane-bound protein measures neutron reflectivity for proteins bound to tethered phospholipid membranes. These methods allow determination of the orientation and shape of membrane-bound proteins. In combination with molecular dynamics simulations, these studies will provide crucial structural information that can serve as a foundation for our understanding of PTEN regulation in normal and pathological processes.

Keywords

phosphoinositide; lipid; membrane; PTEN; phosphatase

7.1 Introduction

The functional diversity of cellular membrane compartments in eukaryotic cells requires that distinct membranes have distinct recognizable surface compositions, comprised of lipid headgroups that are presented to targets in the cytoplasm. Phosphoinositides are phosphorylated derivatives of phosphatidylinositol, which vary in the number and

Corresponding Author: Dr. Alonzo Ross (alonzo.ross@umassmed.edu).

arrangement of additional phosphate residues around the six carbon inositol ring headgroup [1]. This group of lipids is a minor constituent of most cell membranes, yet has important signaling roles and is required for many cellular processes, including endocytosis, autophagy, remodeling of the actin cytoskeleton, cell growth, and proliferation [2]. Seven phosphoinositides have been described in many divergent eukaryotes, with all combinations of one, two or three phosphates in the 3, 4 and 5 positions of the inositol ring. These seven species have distinct functions and cellular distributions [1], some of which are reviewed in other chapters of this volume. This chapter addresses the functions of $PI(4,5)P_2$, which in most cells is the most abundant phosphoinositide with about one mole percent of the plasma membrane (PM) lipid [3]. $PI(4,5)P_2$ interacts with diverse proteins, in many cases acting to regulate membrane remodeling and trafficking events and in other cases binding or directly regulating specific proteins such as small GTPases and ion channels. This phosphoinositide also acts as a metabolic hub, in that it has multiple routes of synthesis and metabolism and in particular is the substrate for two important signaling enzyme families, Phospholipase C (PLC) and Phosphoinositide 3-Kinase (PI3K).

7.1.1 Routes of $PI(4,5)P_2$ Synthesis and Cellular Localization

Several enzymes produce $PI(4,5)P_2$, with the major route of synthesis seemingly mediated by the PIP5K group of phosphoinositide kinases (Figure 1), that phosphorylate PI(4)P [4]. An alternative route of synthesis is from PI(5)P by the PIP4K enzymes. However, cellular levels of PI(5)P are usually far lower than those of PI(4)P, and current data imply that the function of the PIP4K enzymes is more dedicated to the removal of PI(5)P than the generation of $PI(4,5)P_2$ [5, 6]. $PI(4,5)P_2$ is also produced by dephosphorylation of $PI(3,4,5)P_3$ by PTEN. However, since most, if not all, $PI(3,4,5)P_3$ is produced by class I PI3K from the far larger cellular $PI(4,5)P_2$ pool and turns over rapidly, it seems unlikely that the action of PTEN generates functionally significant pools of $PI(4,5)P_2$. The three isoforms of PIP5K that generate $PI(4,5)P_2$ have overlapping but distinct cellular distributions. All are enriched on the PM, but additionally, PIP5Kα is enriched at sites of membrane remodeling such as lamellipodia and nascent phagosomes, PIP5Kβ, at perinuclear vesicles and at least one spliced form of PIP5Kγ, at focal adhesions and epithelial cell-cell junctions [4, 7–9].

Several experimental approaches show that most cellular $PI(4,5)P_2$ is located in the PM [10–12], and several functions of $PI(4,5)P_2$ imply that the lipid acts as a defining marker for the cell plasma membrane environment. In accordance with this concept, evidence shows that $PI(4,5)P_2$ is rapidly metabolized during endocytosis as membrane is internalized [13, 14]. There has also been accumulating support for models in which $PI(4,5)P_2$ (and other lipids) are clustered into small PM microdomains [15–17]. However, the most enigmatic data regarding $PI(4,5)P_2$ localization imply the existence of a small lipid pool in the nuclear matrix [12, 18–21]. The functions of this and other nuclear phosphoinositide pools and even their physical environment are unclear [18].

7.1.2 Direct $PI(4,5)P_2$-Mediated Regulation of Protein Function and Membrane Recruitment

Many proteins have been identified that bind to $PI(4,5)P_2$ with various degrees of selectivity. In some cases, binding is mediated by dedicated lipid-binding domains, such as the Pleckstrin Homology (PH) domain of PLCδ1 or the eponymous Tubby domain from the human Tubby protein [22]. In the case of PLCδ1, it is likely that the PH domain allows competitive binding between $PI(4,5)P_2$ and the PLCδ1 product, $Ins(1,4,5)P_3$ [11, 23]. However, in many other cases, selective binding to the relatively abundant and highly charged $PI(4,5)P_2$ lipid is provided simply by short stretches of amino acids rich in basic residues [24, 25]. This relatively selective interaction of $PI(4,5)P_2$ with polybasic stretches has been identified in many ion channels, the C-termini of a number of small GTPases, many actin-binding proteins and the PTEN tumor suppressor phosphatase [24, 26, 27].

These $PI(4,5)P_2$-polybasic interactions depend not only upon electrostatics but also a precise spatial coordination of the lipid phosphate groups [28, 29]. The simplest initial interpretation of protein binding to $PI(4,5)P_2$ suggests a role in PM recruitment, in particular for the small GTPases, in which a polybasic motif is often combined with a membrane-targeting lipid modification such as prenylation [24]. However, for some proteins, a more complex interaction affects both localization and activity, for example the actin binding protein, ezrin, and PTEN [26, 30, 31].

7.1.3 $PI(4,5)P_2$ as a Platform for Plasma Membrane Based Lipid Signaling

The PM of eukaryotic cells is the key location that mediates cellular responses to the extracellular environment. $PI(4,5)P_2$ serves as a substrate for two families of enzymes that are acutely activated in response to extracellular stimuli via cell surface receptors, namely phosphoinositide-specific PLC and phosphoinositide 3-kinase (PI3K).

7.1.3.1 Phosphoinositide-Specific Phospholipase C—$PI(4,5)P_2$ is the only phosphoinositide that is efficiently cleaved by PLC to form diacylglycerol (DAG) and $Ins(1,4,5)P_3$, and both cleavage products have significant, independent signaling roles (Figure 1) [32]. The best recognized roles for these PLC products are the ability of $Ins(1,4,5)P_3$ to promote the release of calcium ions from intracellular stores and the recognition of membrane localized DAG by modular C1 domains. Notably, the presence of both tandem C1 domains and a calcium-responsive C2 domain in some members of the Protein Kinase C family, underpins the roles of these enzymes as downstream mediators of signaling initiated by PLC cleavage of $PI(4,5)P_2$ [33]. Humans have 13 different *PLC* genes, which through alternative splicing, encode a very large number of enzyme isoforms that share a conserved catalytic region [34]. The structural diversity of these multi-domain proteins allows the activation of PLC by several different classes of cell surface receptors, including many G protein-coupled receptors (GPCRs) and receptor tyrosine kinases (RTKs). Indeed, it seems likely that more cell surface receptors couple to PLC than to any other intracellular receptor-activated signal transducer [32, 34]. The biological responses to PLC activation are almost always mediated by large changes (>10-fold) in the concentrations of DAG and $Ins(1,4,5)P_3$, which are present at much lower concentrations in cells than $PI(4,5)P_2$. In most cases, PLC activation only modestly reduces cellular $PI(4,5)P_2$ levels. However, maximal activation of receptors that very strongly activate PLC, such as the PAR-1/Thrombin receptor, can transiently deplete $PI(4,5)P_2$ levels by as much as 75%. Even in such cases, $PI(4,5)P_2$ pools recover within tens of seconds or at most a few minutes [35]. However, there is evidence, albeit controversial, that spatial segregation of $PI(4,5)P_2$ pools can result in the local depletion of $PI(4,5)P_2$ by PLC and the selective regulation of targets such as ion channels [17, 36].

7.1.3.2 Class I Phosphoinositide 3-Kinase—The phosphorylation of $PI(4,5)P_2$ by the class I PI3K generates the signaling lipid, $PI(3,4,5)P_3$. Similar to PLCs, PI3Ks have low basal activity, but can be acutely activated by several classes of cell surface receptors. PI3K is most strongly activated by RTKs, in particular the insulin receptor and many growth factor receptors as well as some cytokine and chemokine receptors. Humans have 4 catalytic PI3K isoforms, each of which is approximately 110 kDa in size. They exist in cells as heterodimers, bound to one of several regulatory subunits. These catalytic isoforms differ in the receptor classes by which they are activated, with some activated by tyrosine kinase linked receptors (p110α and p110δ), p110γ activated by GPCRs and the p110β isoform activated by phosphotyrosine-based recruitment or GPCRs [35, 37]. The PI3K signaling system has been intensively studied because it is a strong driver of cell proliferation, growth and survival, along with associated changes in metabolism. The PI3K pathway is also activated in many, perhaps most, cancers [38]. One mechanism of oncogenic activation is

via mutations that activate PI3K activity either directly or by the activation of upstream proteins that themselves stimulate PI3K, such as RTKs or Ras. Another, similarly significant mechanism by which PI3K pathway activation occurs in tumors is loss of function of the $PI(3,4,5)P_3$ phosphatase, PTEN. This tumor suppressor protein will be the focus of the rest of this chapter, as it is an excellent example of $PI(4,5)P_2$ regulation, *i.e.*, promoting PTEN activity on the plasma membrane by localizing and directly activating the phosphatase.

7.2 PTEN: A Lipid Phosphatase and $PI(4,5)P_2$-Binding Protein

PTEN is a phosphatidylinositol phosphate (PIP) phosphatase that is specific for the 3-position of the inositol ring [39]. Even though PTEN can dephosphorylate PI(3)P, $PI(3,4)P_2$, and $PI(3,4,5)P_3$ *in vitro* [40], it is likely that $PI(3,4,5)P_3$ is the principal substrate *in vivo*. $PI(3,4,5)P_3$ affects many cellular processes by inducing phosphorylation and activation of the Akt kinase [41–3]. In addition, PTEN may dephosphorylate itself [44].

PTEN has two major structural domains, the phosphatase and C2 domains (Figure 2) [45]. The C2 domain binds anionic lipids, such as phosphatidylserine (PS), independent of Ca^{2+}. In addition, there is a $PI(4,5)P_2$-binding domain at the N-terminus and the phosphatase domain binds the substrate, $PI(3,4,5)P_3$ [26, 40, 46]. There is a C-terminal tail that when phosphorylated, negatively affects phosphatase activity by binding to the C2 and phosphatase domains [47, 48]. Finally, the C-terminus includes a PDZ ligand sequence that binds to linker proteins with PDZ domains [49].

In functional terms, PTEN is a unique protein with many critical functions [50]. PTEN is the second most commonly mutated protein in human cancers [51]. PTEN mutations are associated with autism and macrocephaly [52–8]. In the plant *Arabidopsis*, PTEN is required for pollen maturation [59]. In the slime mold *Dictyostelium discoideum*, PTEN accumulates at the trailing edge of migrating cells and is required for chemotaxis [60]. Honeybee PTEN plays a role in nutrient sensing and queen-worker differentiation [61]. Finally, a PTEN homolog in *Caenorhabditis elegans* worms regulates aging [62].

Given that PTEN plays a role in so many processes, a natural question is whether the PTEN signaling pathways can compensate when something goes wrong with the phosphatase. Mice with one, but not two, PTEN gene knocked out are viable [63]. However, these mice develop a lymphoid hyperplasia and autoimmune disease and display enhanced tumor formation as they age [64]. In fact, substitution of one PTEN gene with a mutant gene with partial activity is sufficient to enhance tumor formation. This result mirrors Cowden's disease in humans born with one intact PTEN gene develop multiple hamartomas [65].

Can we compensate for a deficit in PTEN activity? Because PTEN mostly exists as a phosphorylated proenzyme-like protein with a closed conformation in the cytoplasm [47, 66], it may be possible to activate this reserve pool of soluble PTEN. We are just beginning to understand the equilibrium between soluble and membrane-bound PTEN [67, 68]. A better understanding of the binding of PTEN to $PI(4,5)P_2$ in membranes may allow us to activate PTEN and, thereby, reduce the risk of tumor recurrence.

7.2.1 Anionic Lipids and PTEN Phosphatase Activity

Interactions with cell membranes, notably the PM, likely regulate PTEN phosphatase activity by several mechanisms. Binding of PTEN to biological membranes is dominated by anionic lipids, including PS and $PI(4,5)P_2$ [45, 69, 70]. First, anionic lipids recruits PTEN to the surface of the membrane, where it can laterally diffuse until it encounters the substrate, $PI(3,4,5)P_3$, and hydrolyzes several molecules before returning to the cytoplasm [67]. $PI(3,4,5)P_3$ is present in very low quantities in the membrane and, hence, in the absence of

PS and $PI(4,5)P_2$, would be unlikely to mediate the initial membrane binding. Furthermore, anionic lipids influence the dissociation rate from the membrane. Compared to individual anionic lipids, the combination of PS and $PI(4,5)P_2$ leads to much longer membrane residency [71]. Second, binding of $PI(4,5)P_2$ to the PTEN N-terminal domain increases phosphatase activity [26, 48, 72]. These studies were carried out with short chain PI phosphates used below their critical micelle concentrations. $PI(4,5)P_2$, and to a lesser degree PI(5)P, activated the phosphatase activity [26]. Another interfacial enzyme, phospholipase A_2, also undergoes conformational changes upon membrane binding [73–5]. Myotubularin is a PIP phosphatase that dephosphorylates $PI(3,5)P_2$ [76]. It is intriguing that similar to PTEN, the product, PI(5)P, activates myotubularin. Anionic lipids may also create asymmetric distributions of PTEN. Devreotes and coworkers showed that PTEN is localized in the trailing edge of migrating cells [77]. Also, the distribution of anionic lipids is dynamic and can be perturbed by physiologic processes, such as phagocytosis in macrophages [78].

7.3 PTEN Binding to Anionic Lipids and Its Function in Creating Phosphoinositide Gradients in Cells

PTEN binds to the membrane through at least two major lipid binding sites: PTEN's N-terminal end binds to $PI(4,5)P_2$, while a stretch of basic amino acids in the CBR3 loop of the C2 domain interacts with PS in a Ca^{2+} independent manner. Binding of anionic lipids, particularly $PI(4,5)P_2$, can principally contribute to PTEN membrane association, however, binding of $PI(4,5)P_2$ to the phosphatase active site must be weak enough so that $PI(4,5)P_2$ can be easily replaced by $PI(3,4,5)P_3$ and the produced (or previously bound) $PI(4,5)P_2$ can be cleared out of the active site.

PTEN's N-terminal end preferentially interacts with $PI(4,5)P_2$, *i.e.*, binding to other phosphoinositide derivatives, including those that carry a similarly high negative charge like $PI(4,5)P_2$, ($PI(3,5)P_2$, $PI(3,4)P_2$, or $PI(3,4,5)P_3$) [79], is significantly weaker [29]. This observation suggests that the interaction between $PI(4,5)P_2$ and PTEN's N-terminal end involves both electrostatics and hydrogen bond formation, apparently, requiring a distinct phosphoinositide headgroup geometry. It has been found that the interaction of PTEN's N-terminus and $PI(4,5)P_2$ triggers a conformational change towards slightly increased α-helical secondary structure elements. At first glance one might expect that this structural change is localized at PTEN's N-terminal end, however, infrared spectroscopy measurements utilizing a peptide derived from PTEN's N-terminal end that exhibits the same $PI(4,5)P_2$ binding preference as the full length protein showed that this part of the PTEN protein in all likelihood remains unstructured upon interaction with $PI(4,5)P_2$ [29].

A truncated $PTEN_{16–403}$ protein did not show activity towards $PI(3,4,5)P_3$ embedded in a lipid bilayer [26], consistent with *in vivo* experiments that showed reduced or no membrane association [46] and with *in vitro* measurements that showed strongly reduced binding to $PC/PI(4,5)P_2$ mixed vesicles. $PTEN_{12–16}$ (NKRRY) is highly conserved across different species and among various phosphoinositide phosphatases, such as Ci-VSP, TPTE and TPIP (*Ciona intestinalis* Voltage Sensing Phosphatase, Transmembrane phosphatase with tensin homology, and TPTE and PTEN homologous inositol lipid phosphatase). In addition, the cancer relevant K13E PTEN mutant does not bind to $PI(4,5)P_2$-containing model membranes [29]. It appears that not only the proper lipid headgroup geometry is an important factor for the interaction between PTEN and phosphoinositides, but that this distinct headgroup geometry requires an equally distinct amino acid sequence (*i.e.*, reversing the sequence of adjacent amino acids affects binding; Redfern, Ross, Gericke, unpublished results). It is likely that R11 and K6 participate in the binding, however, it is unresolved whether these amino acids merely provide a suitable electrostatic environment or participate more directly in the binding event.

The C2 domain has been shown to interact with PS through a lysine-rich string of amino acids (PTEN residues 259–269) in the CBR3 loop. Alanine mutations of lysine residues in this region led to a significantly reduced binding of PTEN to PS-containing model membranes [69]. It is important to note that the interaction of PTEN with PS (C2 domain) and $PI(4,5)P_2$ (N-terminal end) is synergistic rather than competitive [29, 71].

PTEN association with the membrane is dynamic. Single molecule TIRF microscopy measurements [67] showed the enzyme binds to the membrane for a few hundred milliseconds, which is a time frame that allows the protein to dephosphorylate several $PI(3,4,5)P_3$ molecules. The mechanisms (or reasons) that cause the protein to dissociate from the membrane are largely unknown at this point.

While mutations in these primary lipid-binding modules lead to a reduced membrane association, other mutations have been reported to increase lipid binding and membrane association. The autism-related H93R PTEN mutation exhibited in *in vitro* experiments enhanced binding to PS containing (but not $PI(4,5)P_2$) model membranes [71, 80] and *in vivo* experiments revealed a significantly increased PM localization in comparison to wild-type PTEN [80]. Surprisingly, this enhanced membrane association did not translate into increased overall activity, but rather the opposite was observed. Similarly, the PTEN E307K mutant was present in higher concentrations in the membrane fraction, however, also in this case, this enhanced membrane association did not translate into an overall higher activity (the activity was largely unchanged in comparison to wild type PTEN) [72].

$PI(3,4,5)P_3$ has been associated with cytoskeletal rearrangements and the PI3K/PTEN enzyme system has been found to play an important role in the regulation of phosphoinositide gradients in migrating cells and during cytokinesis [81, 82]. The Devreotes group investigated the role of $PI(3,4,5)P_3$ gradients in chemotaxis [77, 83, 84]. For migrating *D. discoideum* cells, they found elevated $PI(3,4,5)P_3$ levels at the leading edge of the migrating cell, while at the trailing end $PI(3,4,5)P_3$ levels were depleted. Correspondingly, PI3K and PTEN accumulated at the leading edge and trailing end of the cells, respectively. This functional role of PTEN was mirrored in HL60 cells, a cell line that can be differentiated in neutrophil-like cells *in vitro* [85]. However, *pten*$^{-/-}$ neutrophils did not show elevated $PI(3,4,5)P_3$ levels. In this case, the 5-phosphatase SHIP1 (SH2 domain containing inositol 5-phosphatase 1) was found to be essential for maintaining the $PI(3,4,5)P_3$ gradient [86].

Phosphorylation/dephosphorylation at the C-terminal end (S380, T382, T383, and S385) has been identified as an important regulator for PTEN's competency to bind to membranes. Vazquez *et al.* [47, 66] proposed a phosphorylation-dependent open/closed model for PTEN. In this model, which was recently verified by Radhar *et al.* [68], the phosphorylated C-terminal end folds back onto the phosphatase domain, presumably with one of the phosphorylated amino acids acting as a pseudo-substrate. Independent of tissue, it appears that almost all cellular PTEN is phosphorylated on some or all of these residues [87, 88] and (Maccario and Leslie, unpublished).

7.3.1 Voltage-Sensitive Phosphatases

Voltage-sensitive phosphatases (VSP) and PTEN may be regulated by related mechanisms [89]. The VSP from the sea squirt *Ciona intestinalis* (Ci-VSP) (mentioned above) was the first member of this family to be characterized. This protein has a voltage-sensing domain and PTEN-like phosphatase domain with 5'-phosphatase voltage-dependent activity [90]. Remarkably, a hybrid protein with the Ci-VSP voltage-sensing domain and human PTEN-like phosphatase domain show voltage-dependent phosphatase activity [91]. Furthermore, the linker region appears to play a critical role in this regulation [92, 93], as it may bind

$PI(4,5)P_2$, followed by a voltage-dependent conformational change in the Ci-VSP phosphatase domain [94, 95]. A detailed comparison of the regulation of PTEN and Ci-VSP may allow us to better understand both enzymes.

7.4 Structure of Membrane-Bound PTEN

Attempts to enhance PTEN activity are hindered by the paucity of data on the structure of membrane-bound PTEN. The structure of membrane-bound peripheral proteins are difficult to obtain on physiologically relevant, thermally disordered membranes, because x-ray crystallography is not compatible with the disordered state of the membrane. NMR techniques only provide a window into local contacts, making it difficult to investigate large protein-membrane complexes. However, neutron reflectometry (NR) [96] of PTEN bound to substrate-supported bilayers recently provided a first glimpse into the interaction of this phosphatase with bilayer surfaces and has led to a low-resolution structure [71]. This structure has subsequently been refined and characterized in more detail with all-atom MD simulations (Shenoy et al., submitted).

An interesting new twist on the membrane binding of PTEN comes from a recent report by Huang and coworkers [97] who presented evidence that SUMOylation of the protein is essential to recruit the phosphatase to the membrane. There are two SUMOylation sites, K254 and K266, but the K266 site is more influential. They carry out MD simulations of a PTEN-SUMO hybrid in solution from which they suggest that SUMO acts as an electrostatic adhesion promoter. Despite an impressive amount of data, there remain several important questions. First, bacterial recombinant PTEN lacking SUMOylation binds to membranes and is active [29]. Moreover, two K266 mutants showed normal activity in a U87MG cell model [98]. Second, even though they conclude that the SUMOylation is essential for tumor suppressor activity, there are no cancer-associated mutations of SUMOylation site K266 in the Sanger Center Cosmic Database (http://www.sanger.ac.uk/genetics/CGP/cosmic/). Third, we have carried out extensive MD studies of PTEN and anionic membranes (Shenoy et al, submitted) and find PTEN-membrane interactions consistent with our binding studies and NR analysis, *i.e.*, these simulations suggest PTEN readily associates with the membrane surface without a SUMO modification. Resolution of this controversy requires additional biophysical characterization of PTEN-membrane interactions.

7.4.1 Experimental Approaches

Recent developments in membrane-mimetic model systems [99, 100] facilitate structural investigations of membrane-associated proteins in sample environments that capture the relevant features of biological membranes in highly simplified, well-controlled formats. The original designs of substrate-supported, planar bilayer membranes [101, 102] have been considerably refined in the past decade [100, 103–106], as it was realized that the chemical ‘tethering’ of membranes to an underlying substrate increases the robustness of the resulting model systems [107]. Systems have been reported in which bilayers are decoupled from solid supports by ultrathin, hydrated polymer cushions [108–111] or short linear tethers of hydrophilic oligomers [112–114]. Both tethering approaches lead to the stabilization of well-defined hydrated cushion layers between membrane and carrier substrate [113], important to maintain in-plane fluidity of the bilayers, to protect the protein from denaturation or aggregation following unspecific adsorption to the otherwise bare substrate surface and to permit the incorporation of transmembrane proteins [115–117]. A system developed in the Lösche group [113], the sparsely-tethered bilayer lipid membrane (stBLM), is widely applicable for the biophysical characterization of lipid-protein interactions and is particularly useful for high-resolution neutron scattering investigations [115, 118]. Thiolated tether lipids [113, 114], laterally diluted by coadsorption with β-mercaptoethanol to

atomically flat gold films supported by Si or glass substrates, are used to anchor bimolecular phospholipid films. The lipid bilayers in stBLMs are essentially defect-free and hence highly insulating [113, 119], as shown with electrochemical impedance spectroscopy [120]. Any bilayer platform that is used to study lipid-protein interactions by NR must be stable for the duration of the experiment and at the same, must mirror the in-plane fluidity of biological membranes. To combine both of these aspects in one model system has been a challenge for many years and arguably, stBLMs meet this crucial requirement like no other lipid model system:

1. Phospholipid bilayers in stBLMs are thermally disordered, exhibit in-plane fluidity and hence, resemble biological membranes in these aspects. Adsorbed peripheral proteins or incorporated membrane-spanning proteins [115] therefore reside in a near-natural environment. In fact, fluidity of the stBLMs leads to biological activities of associated proteins similar to those observed in biological membranes, as shown by measuring enzymatic turnover as a function of chain composition [121].

2. The resilience of stBLMs permits *in situ* manipulation of the sample, such as the exchange of the fluid buffer bathing the bilayer for isotopic contrast variation [113, 115]. This capability permits multiple subsequent NR measurements on the same physical sample. stBLMs, therefore, can be measured as neat bilayers, prior to protein incubation, with the protein adsorbed, and after a final rinse, with all measurements performed at a standardized series of $^{1}H_2O/^{2}D_2O$ buffer compositions. Thereby, even though the number of adjustable parameters in the NR experiments is large, this model system is still overdetermined because of multiple NR spectra independently measured with varying conditions. For example, it has been shown that the position of a protein reconstituted in the bilayer membrane can be determined with ≈ 1 Å precision if the internal structure of the protein is known [115].

3. The same lipid model system can be used for a variety of characterization techniques, such as surface plasmon resonance (SPR) [122] and electrochemical impedance spectroscopy [120] if the gold film that covers the carrier substrate is sufficiently thick (typically 100 nm). Fluorescence microscopy and fluorescence correlation spectroscopy (FCS), as well as NR, are compatible with thin gold films (typically 10 nm).

Neutron (or x-ray) scattering – in distinction to diffraction, which requires ordered molecular arrays as in a protein crystal – has the capability to characterize intrinsically disordered samples, including disordered membranes. NR and x-ray reflectometry are surface-sensitive variants of the generic scattering process that take advantage of the refraction and reflection of a beam directed toward an interface. These techniques are therefore particularly sensitive to the molecular structure near surfaces and interfaces. Their physical principles have been exhaustively covered. Significantly, because of the lack of phase information, the molecular structures that give rise to the scattering are most conveniently described in models whose parameters are adjusted to fit the experimentally observed results [96, 118, 123, 124]. In *specular* reflection, where incoming and outgoing wave vectors, $\vec{k}_{in}$ and $\vec{k}_{out}$ have the same overall length and in-plane component, the generic output of such models are scattering length density (SLD) profiles, *i.e.*, projections on the surface normal z of the three-dimensional scattering length distributions.

For samples such as the stBLMs used to investigate protein interactions with phospholipid bilayers, the interfacial structure of the membrane system and its carrier in the absence on any protein is already fairly complex in the absence of any protein. A typical sample consists of a Si wafer that bears a sputtered chromium bonding layer and a terminal Au film

(Figure 3). Chemisorbed to the gold surface is a mixed monolayer of β-mercaptoethanol and thiolated oligo(ethyleneoxide) lipid. The lipid's hydrophobic chains intercalate the phospholipid leaflet proximal to the gold surface, thus tethering the membrane to the substrate, and the bilayer is terminated with a distal phospholipid monolayer.

Molecular dynamics (MD) simulations of wild-type PTEN were performed with the protein deeply embedded in buffer (≈ 74,000 TIP3P water molecules) and on a large patch of PC/PS bilayer membrane (≈ 104,000 TIP3P water and 648 lipid molecules). The CHARMM22/CMAP and CHARMM36 parameterizations were used for the protein and lipid, respectively. Protein conformations started in the crystal structure of the truncated protein [45] with the clipped protein regions added back in energy-minimized conformations. The long (52 residues) C-terminal stretch was initially artificially extended into the buffer from the protein body, and the compact protein domains were located > 10 Å away from the membrane surface in roughly the expected orientation for membrane binding. Simulated annealing procedures were applied to equilibrate these initial structures followed by production runs in excess of 300 ns duration (Shenoy et al., submitted).

7.4.2 PTEN Affinity for Anionic Membranes

Used as biomimetic surfaces in SPR to quantify protein affinity to membranes, stBLMs have low unspecific protein adsorption because stBLMs exhibit low defect densities [71]. In a recent study of PTEN interactions with anionic stBLMs, we reported that the wild-type protein binds to PS-containing membranes with a dissociation constant, $K_d = 11.9 \pm 0.4$ μM, with binding curves evaluated as Langmuir isotherms. For membranes that contained $PI(4,5)P_2$ but no PS, $K_d = 0.4 \pm 0.1$ μM. stBLMs that contain both PS and $PI(4,5)P_2$ show pronounced synergy in protein binding and increased protein affinity by another order of magnitude. In three-component systems (PC:PS:$PI(4,5)P_2$ with the $PI(4,5)P_2$ as a minority component in the 1–3 mol% range), binding curves were reported to be bimodal with one $K_d = 40 \pm 10$ nM and another $K_d > 5$ μM, with the latter value similar to that observed for stBLMs with PS as the sole anionic component. In all cases, protein loading depends on the amount of anionic lipid in the membrane, whereas K_d does not. Specifically, bilayers that included 30 mol% DOPS in DOPC, with or without $PI(4,5)P_2$, were observed to bind wild-type PTEN in amounts ($B_{max} > 150$ ng/cm^2) consistent with the formation of a fairly densely packed monolayer of the protein that may be suitable for investigations with NR. Protein binding depended pronouncedly on bilayer fluidity. While the K_d value reported above ($K_d = 0.4 \pm 0.1$ μM) refers to stBLMs composed of lipids with unsaturated acyl chains (dioleoyl for PC and PS and purified natural $PI(4,5)P_2$), the affinity was at least a factor of 5 lower ($K_d \approx 2$ μM) to stBLMs composed of DPPC and $DPPI(4,5)P_2$.

7.4.3 PTEN Density Distribution on stBLMs by Neutron Reflectometry

NR results for PTEN bound to bilayers composed of PC and PS, as well as PC and $PI(4,5)P_2$, were recently reported for the wild-type protein and the H93R mutant, which is associated with autism [71]. Subsequently, all-atom MD simulations of membrane-bound wild-type PTEN were reported and complemented with simulations of the protein in buffer (Shenoy et al, submitted). Because the simulations have so far not included $PI(4,5)P_2$, we concentrate in this review on the structure of wild-type PTEN on PC/PS-containing bilayers and show how the combination of NR with MD results yields a reference structure for this important phosphatase on a fluid, thermally disordered membrane.

NR spectra were measured first for the pristine stBLM and then for the same lipid bilayer after protein binding. Since all data were collected on one physical sample, the spectra could be modeled with one consistent framework in which many parameters, for example those that describe the multilayered carrier structure, were shared between spectra. Because the

structure of the membrane-bound PTEN protein is *a priori* unknown, its contribution to the overall neutron SLD (nSLD) profile was fitted with a set of spline functions. While these protein contributions were allowed to penetrate the bilayer structure, it was observed that they are only peripherally associated with the membrane surface in models that are consistent with the experimental data (Figure 4). The nSLD profile can be further interpreted to yield a tentative structure of the protein–membrane complex. The crystal structure of the truncated PTEN protein (from which residues 1–6, 286–309, and 354–403 are missing and a few more, residues 7–13, 282–285, and 352–353, are not resolved) could be placed on the membrane model in the orientation proposed by Lee and coworkers [45] and its projection scaled and overlaid on the experimental nSLD profile (dashed line in Figure 4). This procedure provides an astounding agreement between the two projections in the region close to the bilayer surface (z = 0–35 Å in Figure 4, where the z axis originates at the membrane surface), while the region further away (z = 35–60 Å) shows significantly higher nSLD, attributed to the PTEN protein, in the experimental profile. It was suggested [71] that the discrepancy between these densities is due to the truncations for the PTEN protein used for the crystal structure – most notably the C-terminal tail that constitutes the major part of the clipped protein sections, ≈ 20% of the total weight, and is predominantly anionic with 10 excess negative charges. It is then tempting to speculate that electrostatic repulsion keeps the unstructured, presumably flexible anionic C-terminal tail away from the acidic membrane surface. An inset in Figure 4 shows a schematic visualization of the structure of wild-type PTEN on the bilayer that is consistent with the data and displays the C-terminal tail in hypothetic conformations generated with a Monte-Carlo procedure [125]. In conclusion, the NR data on wild-type PTEN on a PC/PS bilayer in connection with the crystal structure [45] of the truncated protein suggest that (1) PTEN scoots on the membrane, (2) the crystal structure is indeed a good starting point for an atomic-scale interpretation and (3) that the C-terminal tail is tugged away from the bilayer surface in the membrane-bound protein [71].

7.4.4 MD Simulations and Their Correspondence with NR Results

Subsequent to the NR investigations reviewed above, all-atom MD simulations of wild-type PTEN were performed on PC/PS bilayers and in solution (Shenoy et al., submitted). Simulations of the membrane-bound PTEN (PC:PS = 2:1, as compared to a 7:3 mixture in the NR experiments) were initiated with the protein > 10 Å distant from the bilayer surface, and it settled quickly into a more stable position with the protein close to the lipid/buffer interface. At the same time the C-terminal tail, which pointed away from the protein core and the membrane initially, contracted and settled in a compact, yet highly dynamic conformation located near the face of the protein body that is distal to the membrane surface. The organization of the two core domains, C2 and phosphatase domain, and their mutual arrangement was conserved in the MD protein structure on the membrane but deviated slightly from the crystal structure. Overall, these deviations were too small to be resolved in NR measurements. Figure 4 compares the nSLD profiles derived from the averaged projections of the full-length protein on the local z axis as seen in the MD simulations with those derived from NR. Various partial protein components, *i.e.* the C-terminal tail, the phosphatase domain, and C2, as well as the sum of the two core domains as a visualization of a dynamic projection of the protein's truncated crystal structure are also shown in the panel. It is evident that the overall protein nSLDs derived from the simulations and from NR experiments corresponded to each other extremely well. The only adjustable quantity in this comparison was the amount of protein per unit area, which was different in both situations. On the one hand, this suggested that the parameterizations of both the protein and the lipid have matured to a performance where they can reproduce experimental situations without any "steering", even for highly charged bilayers. On the other hand, the observed correspondence corroborated the tentative interpretations of the NR results discussed in the previous section. In other words, the experimental and simulation results

cross-validate each other and provide confidence in a reference structure of a partially disordered phosphatase protein associated with a thermally disordered lipid membrane at Ångstrom resolution.

Indeed, the MD simulations provided atomic-scale insight into structure and interactions of the protein with the membrane, and complementing simulations of full-length PTEN in buffer revealed important structural differences of the protein in these distinct environments (Shenoy et al., submitted).

1. While the C2 domain led the docking of the core protein to the charged membrane by penetrating the lipid headgroups locally with its CBR3 loop and anchoring the protein firmly, there were also transient electrostatic interactions observed between the phosphatase domain and charged lipid headgroups. Electrostatic interactions provided the driving force for protein anchoring between a patch of cationic residues on CBR3 and PS, but hydrophobic contacts between M264 and K265 and PS glycerol backbones reinforced these interactions. As a result, specific PS–C2 contacts prevailed for the entire duration of the MD trajectory (> 300 ns). In distinction, electrostatic contacts between PS and the phosphatase domain were more dynamic, lasting only tens of nanoseconds in the simulation.
2. Lipid diffusion was severely restricted by PTEN binding. While the diffusion coefficient derived from the simulation was $D = 7.5\ \mu m^2/s$ for phospholipids in the absence of protein, it was reduced to $3\ \mu m^2/s$ and $1.5\ \mu m^2/s$ for DOPC and DOPS, respectively, for lipids in the footprint of the protein.
3. The simulation also suggested that both the solution and the membrane-bound structures of the PTEN core differ slightly from the published crystal structure. While the solution structure was on average slightly more closed, the protein flattened upon binding to the membrane surface, thus locating the substrate-binding pocket closer to the lipid headgroups. An analysis of the flexibility of the protein core suggested that the phosphatase domain's pα1 helix is the hot spot of displacements with average deviations of the Cα positions of > 3 Å from those in the crystal structure (Shenoy et al., submitted). Generally, the observed deviations from the crystal structure are too small to be resolved in NR measurements.
4. The most significant difference between the solution and membrane-bound structures of wild-type PTEN concerned the C-terminal tail and provided a functional scenario that might implement a control mechanism of the membrane binding of the phosphatase, and hence of its activity (Shenoy et al., submitted). While the tail was displaced from the membrane in the MD simulations, presumably by repulsive electrostatic interactions between the anionic membrane surface and the anionic excess charges on the peptide, it wrapped tightly around the C2 domain in solution, leading to a more compact, globular structure of the protein, as illustrated in representative simulation snapshots shown in Figure 5. The tight "hugging" of the C2 domains leaves the dangling tip of the C-terminus in a position where it obstructs the membrane-binding interface of the core domains. While the conformation of the flexible tail is apparently reversible upon membrane binding of the protein (Figure 5A), it might be locked into place through phosphorylation of the tail. The right hand side of Figure 5B shows various known Thr and Ser phosphorylation sites. In particular S380 and S385 are located on a prominent kink in the tail as it wraps around the C2 domain, suggesting that it could be very well amenable to phosphorylation.

7.4.5 Reference Structure for a Membrane-Bound Phosphatase

Progress in the structural characterization of membrane-bound proteins on thermally disordered, fluid lipid bilayers has been made by combining neutron scattering experiments on dedicated sample formats with all-atom MD simulations. The studies reviewed here provide a reference structure for a phosphoinositide-specific phosphatase and provide a first atomic-scale glimpse into the mechanics of the membrane binding of the PTEN tumor suppressor. Moreover they suggest a mechanism that could provide a control of the membrane association, and therefore the activity, of this important regulatory enzyme in the PI3K/Akt signaling pathway.

7.5 Summary and Future

$PI(4,5)P_2$ is a major component for signaling by several mechanisms. It is the source of $PI(3,4,5)P_3$ and $Ins(1,4,5)P_3$. Furthermore, $PI(4,5)P_2$ is localized in the PM where a number of integral and peripheral membrane proteins can bind it. We have chosen PTEN as an example for this mechanism of regulation. The lack of structural data has been a major impediment in understanding how $PI(4,5)P_2$ activates PTEN. Although just a first step, we summarize how NR can provide structures for membrane-bound proteins in their natural, disordered membrane environment. In combination with NMR and x-ray crystallography, this technique perhaps offers great promises to understand how $PI(4,5)P_2$ controls PTEN activity and, consequently, many downstream physiological processes.

Acknowledgments

We thank Marie-Claire Daou for PTEN protein preparation, and Drs. Siddharth Shenoy, Prabhanshu Shekhar, Frank Heinrich, and Hirsh Nanda for conducting the neutron scattering and MD simulation work and for stimulating discussions and Drs. David Vanderah and Gintaras Valincius for a fruitful collaborations on the design and optimization of tethered bilayer sample formats. This work was supported by the NIH (1P01 AG032131 and RO1 NS021716), NSF (CHEM 442288) and the Department of Commerce (70NANB8H8009 and 70NANB11H8139). Beamtime at the NIST Center for Neutron Research and computational resources at the NIH (http://biowulf.nih.gov), the Extreme Science and Engineering Discovery Environment (XSEDE), supported by the NSF (OCI-105357), with computations performed at the NICS (http://www.nics.tennessee.edu/) and the Pittsburgh Supercomputing Center (BIO110004P), are gratefully acknowledged.

References

1. Di Paolo G, De Camilli P. Phosphoinositides in cell regulation and membrane dynamics. Nature. 2006; 443:651–657. [PubMed: 17035995]
2. Foukas LC, Berenjeno IM, Gray A, Khwaja A, Vanhaesebroeck B. Activity of any class IA PI3K isoform can sustain cell proliferation and survival. Proc. Natl. Acad. Sci. USA. 2010; 107:11381–11386. [PubMed: 20534549]
3. Leslie NR, Downes CP. PTEN: The down side of PI 3-kinase signalling. Cell. Signal. 2002; 14:285–295. [PubMed: 11858936]
4. van den Bout I, Divecha N. PIP5K–driven PtdIns(4,5)P_2 synthesis: regulation and cellular functions. J. Cell Sci. 2009; 122:3837–3850. [PubMed: 19889969]
5. Clarke JH, Irvine RF. The activity, evolution and association of phosphatidylinositol 5-phosphate 4-kinases. Adv. Enzyme Regul. 2012; 52:40–45.
6. Ramel D, Lagarrigue F, Pons V, Mounier J, Dupuis-Coronas S, Chicanne G, Sansonetti PJ, Gaits-Iacovoni F, Tronchère H, Payrastre B. Shigella flexneri infection generates the lipid PI5P to alter endocytosis and prevent termination of EGFR signaling. Sci. Signal. 2011; 4:ra61. [PubMed: 21934107]
7. Doughman RL, Firestone AJ, Wojtasiak ML, Bunce MW, Anderson RA. Membrane ruffling requires coordination between type Iα phosphatidylinositol phosphate kinase and Rac signaling. J. Biol. Chem. 2003; 278:23036–23045. [PubMed: 12682053]

8. Giudici ML, Lee K, Lim R, Irvine RF. The intracellular localisation and mobility of Type Iγ phosphatidylinositol 4P 5-kinase splice variants. FEBS Lett. 2006; 580:6933–6937. [PubMed: 17157843]
9. Ling K, Bairstow SF, Carbonara C, Turbin DA, Huntsman DG, Anderson RA. Type Iγ phosphatidylinositol phosphate kinase modulates adherens junction and E-cadherin trafficking via a direct interaction with μ1B adaptin. J Cell Biol. 2007; 176:343–353. [PubMed: 17261850]
10. Hammond GRV, Schiavo G, Irvine RF. Immunocytochemical techniques reveal multiple, distinct cellular pools of PtdIns4P and PtdIns(4,5)P_2 . Biochem. J. 2009; 422:23–35. [PubMed: 19508231]
11. Szentpetery Z, Balla A, Kim YJ, Lemmon MA, Balla T. Live cell imaging with protein domains capable of recognizing phosphatidylinositol 4,5-bisphosphate; a comparative study. BMC Cell Biol. 2009; 10:67. [PubMed: 19769794]
12. Watt SA, Kular G, Fleming IN, Downes CP, Lucocq JM. Subcellular localization of phosphatidylinositol 4,5-bisphosphate using the pleckstrin homology domain of phospholipase C δ1. Biochem. J. 2002; 363:657–666. [PubMed: 11964166]
13. Nakatsu F, Perera RM, Lucast L, Zoncu R, Domin J, Gertler FB, Toomre D, De Camilli P. The inositol 5-phosphatase SHIP2 regulates endocytic clathrin-coated pit dynamics. J. Cell Biol. 2010; 190:307–315. [PubMed: 20679431]
14. Vicinanza M, Di Campli A, Polishchuk E, Santoro M, Di Tullio G, Godi A, Levtchenko E, De Leo MG, Polishchuk R, Sandoval L, Marzolo M-P, De Matteis MA. OCRL controls trafficking through early endosomes via PtdIns4,5P_2-dependent regulation of endosomal actin. EMBO J. 2011; 30:4970–4985. [PubMed: 21971085]
15. James DJ, Khodthong C, Kowalchyk JA, Martin TFJ. Phosphatidylinositol 4,5-bisphosphate regulates SNARE-dependent membrane fusion. J. Cell Biol. 2008; 182:355–366. [PubMed: 18644890]
16. Lingwood D, Simons K. Lipid rafts as a membrane-organizing principle. Science. 2010; 327:46–50. [PubMed: 20044567]
17. van den Bogaart G, Meyenberg K, Risselada HJ, Amin H, Willig KI, Hubrich BE, Dier M, Hell SW, Grubmüller H, Diederichsen U, Jahn R. Membrane protein sequestering by ionic protein-lipid interactions. Nature. 2011; 479:552–555. [PubMed: 22020284]
18. Barlow CA, Laishram RS, Anderson RA. Nuclear phosphoinositides: A signaling enigma wrapped in a compartmental conundrum. Trends Cell Biol. 2010; 20:25–35. [PubMed: 19846310]
19. Cocco L, Gilmour RS, Ognibene A, Letcher AJ, Manzoli FA, Irvine RF. Synthesis of polyphosphoinositides in nuclei of Friend cells. Evidence for polyphosphoinositide metabolism inside the nucleus which changes with cell differentiation. Biochem. J. 1987; 248:765–770. [PubMed: 2829840]
20. Cocco L, Manzoli L, Barnabei O, Martelli AM. Significance of subnuclear localization of key players of inositol lipid cycle. Adv. Enzyme Regul. 2004; 44:51–60. [PubMed: 15581482]
21. Irvine RF. Nuclear lipid signalling. Nat. Rev. Mol. Cell Biol. 2003; 4:349–360. [PubMed: 12728269]
22. Santagata S, Boggon TJ, Baird CL, Gomez CA, Zhao J, Shan WS, Myszka DG, Shapiro L. G-protein signaling through tubby proteins. Science. 2001; 292:2041–2050. [PubMed: 11375483]
23. Hirose K, Kadowaki S, Tanabe M, Takeshima H, Iino M. Spatiotemporal dynamics of inositol 1,4,5-trisphosphate that underlies complex Ca^{2+} mobilization patterns. Science. 1999; 284:1527–1530. [PubMed: 10348740]
24. Heo WD, Inoue T, Park WS, Kim ML, Park BO, Wandless TJ, Meyer T. PI(3,4,5)P_3 and PI(4,5)P_2 lipids target proteins with polybasic clusters to the plasma membrane. Science. 2006; 314:1458–1461. [PubMed: 17095657]
25. Yeung T, Terebiznik M, Yu L, Silvius J, Abidi WM, Philips M, Levine T, Kapus A, Grinstein S. Receptor activation alters inner surface potential during phagocytosis. Science. 2006; 313:347–351. [PubMed: 16857939]
26. Campbell RB, Liu F, Ross AH. Allosteric activation of PTEN phosphatase by phosphatidylinositol 4,5-bisphosphate. J. Biol. Chem. 2003; 278:33617–33620. [PubMed: 12857747]
27. Falkenburger BH, Jensen JB, Dickson EJ, Suh B-C, Hille B. Phosphoinositides: Lipid regulators of membrane proteins. J. Physiol. (Lond.). 2010; 588:3179–3185. [PubMed: 20519312]

28. Hansen SB, Tao X, MacKinnon R. Structural basis of PIP_2 activation of the classical inward rectifier K^+ channel Kir2.2. Nature. 2011; 477:495–498. [PubMed: 21874019]
29. Redfern RE, Redfern DA, Furgason ML, Munson M, Ross AH, Gericke A. PTEN phosphatase selectively binds phosphoinositides and undergoes structural changes. Biochemistry. 2008; 47:2162–2171. [PubMed: 18220422]
30. Fievet BT, Gautreau A, Roy C, Del Maestro L, Mangeat P, Louvard D, Arpin M. Phosphoinositide binding and phosphorylation act sequentially in the activation mechanism of ezrin. J. Cell Biol. 2004; 164:653–659. [PubMed: 14993232]
31. Leslie NR, Batty IH, Maccario H, Davidson L, Downes CP. Understanding PTEN regulation: PIP_2, polarity and protein stability. Oncogene. 2008; 27:5464–5476. [PubMed: 18794881]
32. Katan M. Families of phosphoinositide-specific phospholipase C: Structure and function. Biochim. Biophys. Acta. 1998; 1436:5–17. [PubMed: 9838022]
33. Oancea E, Meyer T. Protein kinase C as a molecular machine for decoding calcium and diacylglycerol signals. Cell. 1998; 95:307–318. [PubMed: 9814702]
34. Nakamura Y, Fukami K. Roles of phospholipase C isozymes in organogenesis and embryonic development. Physiology (Bethesda). 2009; 24:332–341. [PubMed: 19996364]
35. Batty IH, Downes CP. Thrombin receptors modulate insulin-stimulated phosphatidylinositol 3,4,5-trisphosphate accumulation in 1321N1 astrocytoma cells. Biochem. J. 1996; 317(Pt 2):347–351. [PubMed: 8713057]
36. Gamper N, Shapiro MS. Target-specific PIP_2 signalling: How might it work? J. Physiol. (Lond.). 2007; 582:967–975. [PubMed: 17412762]
37. Vanhaesebroeck B, Stephens L, Hawkins P. PI3K signalling: The path to discovery and understanding. Nat. Rev. Mol. Cell Biol. 2012; 13:195–203. [PubMed: 22358332]
38. Yuan TL, Cantley LC. PI3K pathway alterations in cancer: Variations on a theme. Oncogene. 2008; 27:5497–5510. [PubMed: 18794884]
39. Maehama T, Dixon JE. The tumor suppressor, PTEN/MMAC1, dephosphorylates the lipid second messenger, phosphatidylinositol 3,4,5-trisphosphate. J. Biol. Chem. 1998; 273:13375–13378. [PubMed: 9593664]
40. McConnachie G, Pass I, Walker SM, Downes CP. Interfacial kinetic analysis of the tumour suppressor phosphatase, PTEN: Evidence for activation by anionic phospholipids. Biochem. J. 2003; 371:947–955. [PubMed: 12534371]
41. Datta SR, Brunet A, Greenberg ME. Cellular survival: a play in three Akts. Genes Dev. 1999; 13:2905–2927. [PubMed: 10579998]
42. Stocker H, Andjelkovic M, Oldham S, Laffargue M, Wymann MP, Hemmings BA, Hafen E. Living with lethal PIP_3 levels: Viability of flies lacking PTEN restored by a PH domain mutation in Akt/PKB. Science. 2002; 295:2088–2091. [PubMed: 11872800]
43. Bayascas JR, Leslie NR, Parsons R, Fleming S, Alessi DR. Hypomorphic mutation of PDK1 suppresses tumorigenesis in $PTEN^{+/-}$ mice. Curr. Biol. 2005; 15:1839–1846. [PubMed: 16243031]
44. Zhang XC, Piccini A, Myers MP, Van Aelst L, Tonks NK. Functional analysis of the protein phosphatase activity of PTEN. Biochem. J. 2012; 444:457–464. [PubMed: 22413754]
45. Lee JO, Yang H, Georgescu MM, Di Cristofano A, Maehama T, Shi Y, Dixon JE, Pandolfi PP, Pavletich NP. Crystal structure of the PTEN tumor suppressor: Implications for its phosphoinositide phosphatase activity and membrane association. Cell. 1999; 99:323–334. [PubMed: 10555148]
46. Iijima M, Huang YE, Luo HR, Vazquez F, Devreotes PN. Novel mechanism of PTEN regulation by its phosphatidylinositol 4,5-bisphosphate binding motif is critical for chemotaxis. J. Biol. Chem. 2004; 279:16606–16613. [PubMed: 14764604]
47. Vazquez F, Grossman SR, Takahashi Y, Rokas MV, Nakamura N, Sellers WR. Phosphorylation of the PTEN tail acts as an inhibitory switch by preventing its recruitment into a protein complex. J. Biol. Chem. 2001; 276:48627–48630. [PubMed: 11707428]
48. Odriozola L, Singh G, Hoang T, Chan AM. Regulation of PTEN activity by its carboxyl-terminal autoinhibitory domain. J. Biol. Chem. 2007; 282:23306–23315. [PubMed: 17565999]

49. Molina JR, Agarwal NK, Morales FC, Hayashi Y, Aldape KD, Cote G, Georgescu M-M. PTEN, NHERF1 and PHLPP form a tumor suppressor network that is disabled in glioblastoma. Oncogene. 2012; 31:1264–1274. [PubMed: 21804599]
50. Song MS, Salmena L, Pandolfi PP. The functions and regulation of the PTEN tumour suppressor. Nat. Rev. Mol. Cell Biol. 2012; 13:283–296. [PubMed: 22473468]
51. Simpson L, Parsons R. PTEN: Life as a tumor suppressor. Exp. Cell Res. 2001; 264:29–41. [PubMed: 11237521]
52. Goffin A, Hoefsloot LH, Bosgoed E, Swillen A, Fryns JP. PTEN mutation in a family with Cowden syndrome and autism. Am. J. Med. Genet. 2001; 105:521–524. [PubMed: 11496368]
53. Butler MG, Dasouki MJ, Zhou X-P, Talebizadeh Z, Brown M, Takahashi TN, Miles JH, Wang CH, Stratton R, Pilarski R, Eng C. Subset of individuals with autism spectrum disorders and extreme macrocephaly associated with germline PTEN tumour suppressor gene mutations. J Med Genet. 2005; 42:318–321. [PubMed: 15805158]
54. Boccone L, Dessì V, Zappu A, Piga S, Piludu MB, Rais M, Massidda C, De Virgiliis S, Cao A, Loudianos G. Bannayan-Riley-Ruvalcaba syndrome with reactive nodular lymphoid hyperplasia and autism and a PTEN mutation. Am J Med Genet A. 2006; 140:1965–1969. [PubMed: 16894538]
55. Herman GE, Butter E, Enrile B, Pastore M, Prior TW, Sommer A. Increasing knowledge of PTEN germline mutations: Two additional patients with autism and macrocephaly. Am J Med Genet A. 2007; 143:589–593. [PubMed: 17286265]
56. Orrico A, Galli L, Buoni S, Orsi A, Vonella G, Sorrentino V. Novel PTEN mutations in neurodevelopmental disorders and macrocephaly. Clin Genet. 2009; 75:195–198. [PubMed: 18759867]
57. Stein MT, Elias ER, Saenz M, Pickler L, Reynolds A. Autistic spectrum disorder in a 9-year-old girl with macrocephaly. J Dev Behav Pediatr. 2010; 31:632–634. [PubMed: 20814261]
58. McBride KL, Varga EA, Pastore MT, Prior TW, Manickam K, Atkin JF, Herman GE. Confirmation study of PTEN mutations among individuals with autism or developmental delays/mental retardation and macrocephaly. Autism Res. 2010; 3:137–141. [PubMed: 20533527]
59. Gupta R, Ting JTL, Sokolov LN, Johnson SA, Luan S. A tumor suppressor homolog, AtPTEN1, is essential for pollen development in Arabidopsis. Plant Cell. 2002; 14:2495–2507. [PubMed: 12368500]
60. Janetopoulos C, Borleis J, Vazquez F, Iijima M, Devreotes PN. Temporal and spatial regulation of phosphoinositide signaling mediates cytokinesis. Dev. Cell. 2005; 8:467–477. [PubMed: 15809030]
61. Mutti NS, Wang Y, Kaftanoglu O, Amdam GV. Honey bee PTEN–Description, developmental knockdown, and tissue-specific expression of splice-variants correlated with alternative social phenotypes. PLoS One. 2011; 6:e22195. [PubMed: 21779392]
62. Ogg S, Ruvkun G. The C. elegans PTEN homolog, DAF-18, acts in the insulin receptor-like metabolic signaling pathway. Mol. Cell. 1998; 2:887–893. [PubMed: 9885576]
63. Di Cristofano A, Kotsi P, Peng YF, Cordon-Cardo C, Elkon KB, Pandolfi PP. Impaired Fas response and autoimmunity in Pten+/− mice. Science. 1999; 285:2122–2125. [PubMed: 10497129]
64. Trotman LC, Niki M, Dotan ZA, Koutcher JA, Di Cristofano A, Xiao A, Khoo AS, Roy-Burman P, Greenberg NM, Van Dyke T, Cordon-Cardo C, Pandolfi PP. Pten dose dictates cancer progression in the prostate. PLoS Biol. 2003; 1:385–396.
65. Eng C, Murday V, Seal S, Mohammed S, Hodgson SV, Chaudary MA, Fentiman IS, Ponder BA, Eeles RA. Cowden syndrome and Lhermitte-Duclos disease in a family: A single genetic syndrome with pleiotropy? J. Med. Genet. 1994; 31:458–461. [PubMed: 8071972]
66. Vazquez F, Ramaswamy S, Nakamura N, Sellers W. Phosphorylation of the PTEN tail regulates protein stability and function. Mol. Cell. Biol. 2000; 20:5010–5018. [PubMed: 10866658]
67. Vazquez F, Matsuoka S, Sellers WR, Yanagida T, Ueda M, Devreotes PN. Tumor suppressor PTEN acts through dynamic interaction with the plasma membrane. Proc. Natl. Acad. Sci. USA. 2006; 103:3633–3638. [PubMed: 16537447]

68. Rahdar M, Inoue T, Meyer T, Zhang J, Vazquez F, Devreotes PN. A phosphorylation-dependent intramolecular interaction regulates the membrane association and activity of the tumor suppressor PTEN. Proc. Natl. Acad. Sci. USA. 2009; 106:480–485. [PubMed: 19114656]
69. Das S, Dixon J, Cho W. Membrane-binding and activation mechanism of PTEN. Proc. Natl. Acad. Sci. USA. 2003; 100:7491–7496. [PubMed: 12808147]
70. Walker S, Leslie N, Perera N, Batty I, Downes C. The tumour-suppressor function of PTEN requires an N-terminal lipid-binding motif. Biochem. J. 2004; 379:301–307. [PubMed: 14711368]
71. Shenoy S, Shekhar P, Heinrich F, Daou M-C, Gericke A, Ross AH, Lösche M. Membrane association of the PTEN tumor suppressor: Molecular details of the protein-membrane complex from SPR binding studies and neutron reflection. PLoS ONE. 2012; 7:e32591. [PubMed: 22505997]
72. Singh G, Odriozola L, Guan H, Kennedy CR, Chan AM. Characterization of a novel PTEN mutation in MDA-MB-453 breast carcinoma cell line. BMC Cancer. 2011; 11:490. [PubMed: 22103913]
73. van den Berg B, Tessari M, Boelens R, Dijkman R, de Haas GH, Kaptein R, Verheij HM. NMR structures of phospholipase A_2 reveal conformational changes during interfacial activation. Nat. Struct. Biol. 1995; 2:402–406. [PubMed: 7664098]
74. Boegeman SC, Deems RA, Dennis EA. Phospholipid binding and the activation of group IA secreted phospholipase A_2 . Biochemistry. 2004; 43:3907–3916. [PubMed: 15049698]
75. Bahnson BJ. Structure, function and interfacial allosterism in phospholipase A_2: Insight from the anion-assisted dimer. Arch. Biochem. Biophys. 2005; 433:96–106. [PubMed: 15581569]
76. Wishart MJ, Dixon JE. PTEN and myotubularin phosphatases: from 3-phosphoinositide dephosphorylation to disease. Trends Cell Biol. 2002; 12:579–585. [PubMed: 12495846]
77. Iijima M, Devreotes PN. Tumor suppressor PTEN mediates sensing of chemoattractant gradients. Cell. 2002; 109:599–610. [PubMed: 12062103]
78. Yeung T, Heit B, Dubuisson J-F, Fairn GD, Chiu B, Inman R, Kapus A, Swanson M, Grinstein S. Contribution of phosphatidylserine to membrane surface charge and protein targeting during phagosome maturation. J. Cell Biol. 2009; 185:917–928. [PubMed: 19487458]
79. Kooijman EE, King KE, Gangoda M, Gericke A. Ionization properties of phosphatidylinositol polyphosphates in mixed model membranes. Biochemistry. 2009; 48:9360–9371. [PubMed: 19725516]
80. Redfern RE, Daou M, Li L, Munson M, Gericke A, Ross AH. A mutant form of PTEN linked to autism. Protein Sci. 2010; 19:1948–1956. [PubMed: 20718038]
81. Cai H, Devreotes PN. Moving in the right direction: How eukaryotic cells migrate along chemical gradients. Semin. Cell Dev. Biol. 2011; 22:834–841. [PubMed: 21821139]
82. Wang Y, Chen C-L, Iijima M. Signaling mechanisms for chemotaxis. Dev. Growth Differ. 2011; 53:495–502. [PubMed: 21585354]
83. Willard SS, Devreotes PN. Signaling pathways mediating chemotaxis in the social amoeba, Dictyostelium discoideum. Eur. J. Cell Biol. 2006; 85:897–904. [PubMed: 16962888]
84. Franca-Koh J, Kamimura Y, Devreotes PN. Leading-edge research: PtdIns(3,4,5)P_3 and directed migration. Nat. Cell Biol. 2007; 9:15–17. [PubMed: 17199126]
85. Weiner OD. Regulation of cell polarity during eukaryotic chemotaxis: The chemotactic compass. Curr. Opin. Cell Biol. 2002; 14:196–202. [PubMed: 11891119]
86. Nishio M, Watanabe K-i, Sasaki J, Taya C, Takasuga S, Iizuka R, Balla T, Yamazaki M, Watanabe H, Itoh R, Kuroda S, Horie Y, Förster I, Mak TW, Yonekawa H, Penninger JM, Kanaho Y, Suzuki A, Sasaki T. Control of cell polarity and motility by the PtdIns(3,4,5)P_3 phosphatase SHIP1. Nat. Cell Biol. 2007; 9:36–44. [PubMed: 17173042]
87. Rabinovsky R, Pochanard P, McNear C, Brachmann SM, Duke-Cohan JS, Garraway LA, Sellers WR. p85 Associates with unphosphorylated PTEN and the PTEN-associated complex. Mol. Cell Biol. 2009; 29:5377–5388. [PubMed: 19635806]
88. Tibarewal P, Zilidis G, Spinelli L, Schurch N, Maccario H, Gray A, Perera NM, Davidson L, Barton GJ, Leslie NR. PTEN protein phosphatase activity correlates with control of gene expression and invasion, a tumor-suppressing phenotype, but not with AKT activity. Sci. Signal. 2012; 5:ra18. [PubMed: 22375056]

89. Villalba-Galea CA. New insights in the activity of voltage sensitive phosphatases. Cell. Signal. 2012; 24:1541–1547. [PubMed: 22481094]

90. Murata Y, Iwasaki H, Sasaki M, Inaba K, Okamura Y. Phosphoinositide phosphatase activity coupled to an intrinsic voltage sensor. Nature. 2005; 435:1239–1243. [PubMed: 15902207]

91. Lacroix J, Halaszovich CR, Schreiber DN, Leitner MG, Bezanilla F, Oliver D, Villalba-Galea CA. Controlling the activity of a phosphatase and tensin homolog (PTEN) by membrane potential. J. Biol. Chem. 2011; 286:17945–17953. [PubMed: 21454672]

92. Hobiger K, Utesch T, Mroginski MA, Friedrich T. Coupling of Ci-VSP modules requires a combination of structure and electrostatics within the linker. Biophys. J. 2012; 102:1313–1322. [PubMed: 22455914]

93. Kohout SC, Bell SC, Liu L, Xu Q, Minor DL, Isacoff EY. Electrochemical coupling in the voltage-dependent phosphatase Ci-VSP. Nat. Chem. Biol. 2010; 6:369–375. [PubMed: 20364128]

94. Matsuda M, Takeshita K, Kurokawa T, Sakata S, Suzuki M, Yamashita E, Okamura Y, Nakagawa A. Crystal structure of the cytoplasmic phosphatase and tensin homolog (PTEN)-like region of Ciona intestinalis voltage-sensing phosphatase provides insight into substrate specificity and redox regulation of the phosphoinositide phosphatase activity. J. Biol. Chem. 2011; 286:23368–23377. [PubMed: 21543329]

95. Liu L, Kohout SC, Xu Q, Müller S, Kimberlin CR, Isacoff EY, Minor DL. A glutamate switch controls voltage-sensitive phosphatase function. Nat. Struct. Mol. Biol. 2012; 19:633–641. [PubMed: 22562138]

96. Schalke M, Lösche M. Structural models of lipid surface monolayers from x-ray and neutron reflectivity measurements. Adv. Colloid Interf. Sci. 2000; 88:243–274.

97. Huang J, Yan J, Zhang J, Zhu S, Wang Y, Shi T, Zhu C, Chen C, Liu X, Cheng J, Mustelin T, Feng G-S, Chen G, Yu J. SUMO1 modification of PTEN regulates tumorigenesis by controlling its association with the plasma membrane. Nat. Commun. 2012; 3:911–922. [PubMed: 22713753]

98. Liu F, Wagner S, Campbell RB, Nickerson JA, Schiffer CA, Ross AH. PTEN enters the nucleus by diffusion. J Cell Biochem. 2005; 96:221–234. [PubMed: 16088943]

99. Cornell BA, Braach-Maksvytis VLB, King LB, Osman PDJ, Raguse B, Wieczorek L, Pace RJ. A biosensor that uses ion-channel switches. Nature. 1997; 387:580–583. [PubMed: 9177344]

100. Tanaka M, Sackmann E. Polymer-supported membranes as models of the cell surface. Nature. 2005; 437:656–663. [PubMed: 16193040]

101. Tamm LK, McConnell HM. Supported phospholipid bilayers. Biophys. J. 1985; 47:105–113. [PubMed: 3978184]

102. Sackmann E. Supported membranes: Scientific and practical applications. Science. 1996; 271:43–48. [PubMed: 8539599]

103. Crane JM, Tamm LK. Role of cholesterol in the formation and nature of lipid rafts in planar and spherical model membranes. Biophys J. 2004; 86:2965–2979. [PubMed: 15111412]

104. Knoll W, Naumann R, Friedrich M, Robertson JWF, Lösche M, Heinrich F, McGillivray DJ, Schuster B, Gufler PC, Pum D, Sleytr UB. Solid supported functional lipid membranes based on monomolecular protein sheet crystals: New concepts for the biomimetic functionalization of solid surfaces. Biointerphases. 2008; 3:FA125–FA135. [PubMed: 20408662]

105. Smith HL, Jablin MS, Vidyasagar A, Saiz J, Watkins E, Toomey R, Hurd AJ, Majewski J. Model lipid membranes on a tunable polymer cushion. Phys. Rev. Lett. 2009; 102:228102. [PubMed: 19658904]

106. Jeuken LJC, Connell SD, Henderson PJF, Gennis RB, Evans SD, Bushby RJ. Redox enzymes in tethered membranes. J. Am. Chem. Soc. 2006; 128:1711–1716. [PubMed: 16448146]

107. Vockenroth IK, Ohm C, Robertson JWF, McGillivray DJ, Lösche M, Köper I. Stable insulating tethered bilayer membranes. Biointerphases. 2008; 3:FA68–FA73. [PubMed: 20408671]

108. Sackmann E, Tanaka M. Supported membranes on soft polymer cushions: Fabrication, characterization and applications. Trends Biotechn. 2000; 18:58–64.

109. Kiessling V, Tamm LK. Measuring distances in supported bilayers by fluorescence interference-contrast microscopy: Polymer supports and SNARE proteins. Biophys. J. 2003; 84:408–418. [PubMed: 12524294]

110. Garg S, Rühe J, Lüdtke K, Jordan R, Naumann CA. Domain registration in raft-mimicking lipid mixtures studied using polymer-tethered lipid bilayers. Biophys. J. 2007; 92:1263–1270. [PubMed: 17114215]
111. Lin J, Szymanski J, Searson PC, Hristova K. Effect of a Polymer Cushion on the Electrical Properties and Stability of Surface-Supported Lipid Bilayers. Langmuir. 2010; 26:3544–3548. [PubMed: 20175577]
112. Purrucker O, Fortig A, Jordan R, Tanaka M. Supported membranes with well-defined polymer tethers-incorporation of cell receptors. ChemPhysChem. 2004; 5:327–335. [PubMed: 15067869]
113. McGillivray DJ, Valincius G, Vanderah DJ, Febo-Ayala W, Woodward JT, Heinrich F, Kasianowicz JJ, Lösche M. Molecular-scale structural and functional characterization of sparsely tethered bilayer lipid membranes. Biointerphases. 2007; 2:21–33. [PubMed: 20408633]
114. Heinrich F, Ng T, Vanderah DJ, Shekhar P, Mihailescu M, Nanda H, Lösche M. A new lipid anchor for sparsely tethered bilayer lipid membranes. Langmuir. 2009; 25:4219–4229. [PubMed: 19714901]
115. McGillivray DJ, Valincius G, Heinrich F, Robertson JWF, Vanderah DJ, Febo-Ayala W, Ignatjev I, Lösche M, Kasianowicz JJ. Structure of functional Staphylococcus aureus α-hemolysin channels in tethered bilayer lipid membranes. Biophys. J. 2009; 96:1547–1553. [PubMed: 19217871]
116. Robelek R, Lemker ES, Wiltschi B, Kirste V, Naumann R, Oesterhelt D, Sinner EK. Incorporation of in vitro synthesized GPCR into a tethered artificial lipid membrane system. Angew. Chem. Int. Ed. Engl. 2007; 46:605–608. [PubMed: 17152105]
117. Sumino A, Dewa T, Takeuchi T, Sugiura R, Sasaki N, Misawa N, Tero R, Urisu T, Gardiner AT, Cogdell RJ, Hashimoto H, Nango M. Construction and structural analysis of tethered lipid bilayer containing photosynthetic antenna proteins for functional analysis. Biomacromolecules. 2011; 12:2850–2858. [PubMed: 21650465]
118. Nanda H, Datta SAK, Heinrich F, Lösche M, Rein A, Krueger S, Curtis JE. Electrostatic interactions and binding orientation of HIV-1 matrix, studied by neutron reflectivity. Biophys. J. 2010; 99:2516–2524. [PubMed: 20959092]
119. Valincius G, Heinrich F, Budvytyte R, Vanderah DJ, McGillivray DJ, Sokolov Y, Hall JE, Lösche M. Soluble amyloid β-oligomers affect dielectric membrane properties by bilayer insertion and domain formation: Implications for cell toxicity. Biophys. J. 2008; 95:4845–4861. [PubMed: 18515395]
120. Valincius G, Meskauskas T, Ivanauskas F. Electrochemical impedance spectroscopy of tethered bilayer membranes. Langmuir. 2012; 28:977–990. [PubMed: 22126190]
121. Valincius G, McGillivray DJ, Febo-Ayala W, Vanderah DJ, Kasianowicz JJ, Lösche M. Enzyme activity to augment the characterization of tethered bilayer membranes. J. Phys. Chem. B. 2006; 110:10213–10216. [PubMed: 16722717]
122. Wiltschi B, Knoll W, Sinner E-K. Binding assays with artificial tethered membranes using surface plasmon resonance. Methods. 2006; 39:134–146. [PubMed: 16857384]
123. Shekhar P, Nanda H, Lösche M, Heinrich F. Continuous distribution model for the investigation of complex molecular architectures near interfaces with scattering techniques. J. Appl. Phys. 2011; 110 102216-102211–102212.
124. Datta SAK, Heinrich F, Raghunandan S, Krueger S, Curtis JE, Rein A, Nanda H. HIV-1 Gag extension: Conformational changes require simultaneous interaction with membrane and nucleic acid. J. Mol. Biol. 2011; 406:205–214. [PubMed: 21134384]
125. Curtis JE, Raghunandran S, Nanda H, Krueger S. SASSIE: A program to study intrinsically disordered biological molecules and macromolecular ensembles using experimental scattering constraints. Comp. Phys. Commun. 2012; 183:382–389.

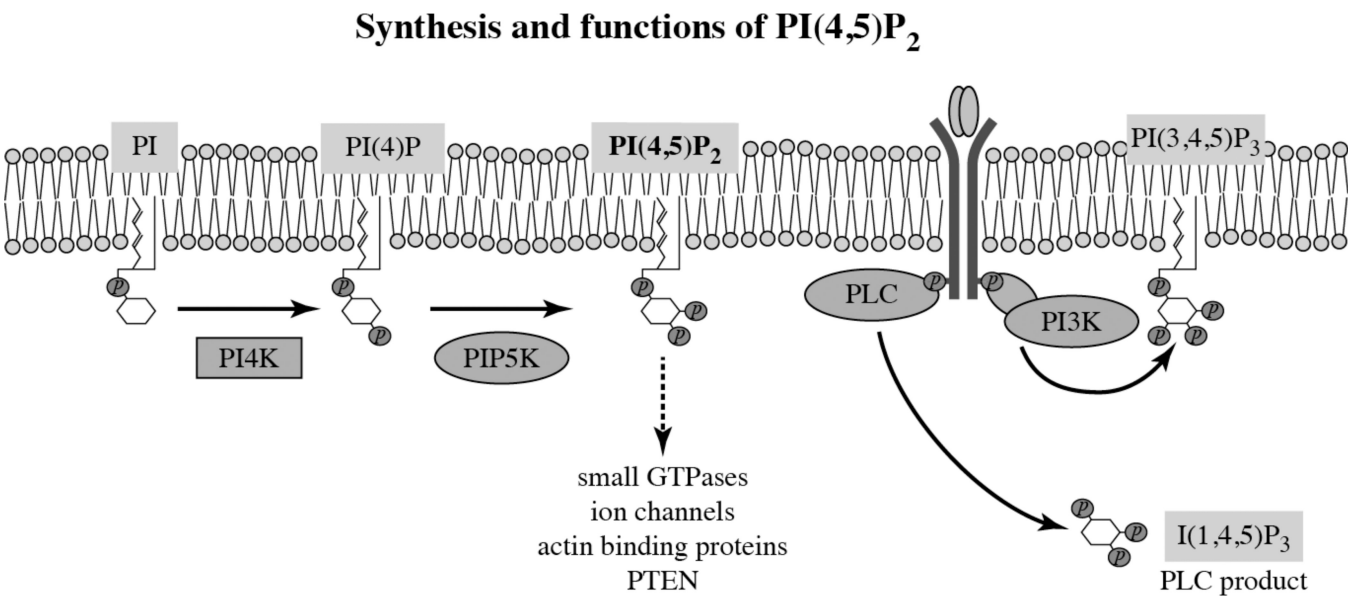

Figure 1.

Synthesis and functions of $PI(4,5)P_2$. The route of synthesis of most cellular $PI(4,5)P_2$ from phosphatidylinositol (PI) via the sequential actions of PI and PI(4)P is shown. Two routes of receptor-stimulated metabolism of $PI(4,5)P_2$ are also shown, being further phosphorylated to PIP3 by class I PI 3-kinase and being cleaved to form IP_3 and diacylglycerol (not shown) by the action of Phospholipase C. For clarity, these reactions are shown within the same membrane compartment, but although all are present on the plasma membrane, PI, PI(4)P and both PI4K and PIP5K activities are abundant on intracellular membranes and the metabolic relationship between these cellular pools is unclear. Some of the recognized functions of $PI(4,5)P_2$ are indicated by a dashed line, reflecting the reversible binding of the lipid to proteins that include many small GTPases of the Ras superfamily, ion channels, actin binding proteins, and the tumor suppressor phosphatase PTEN.

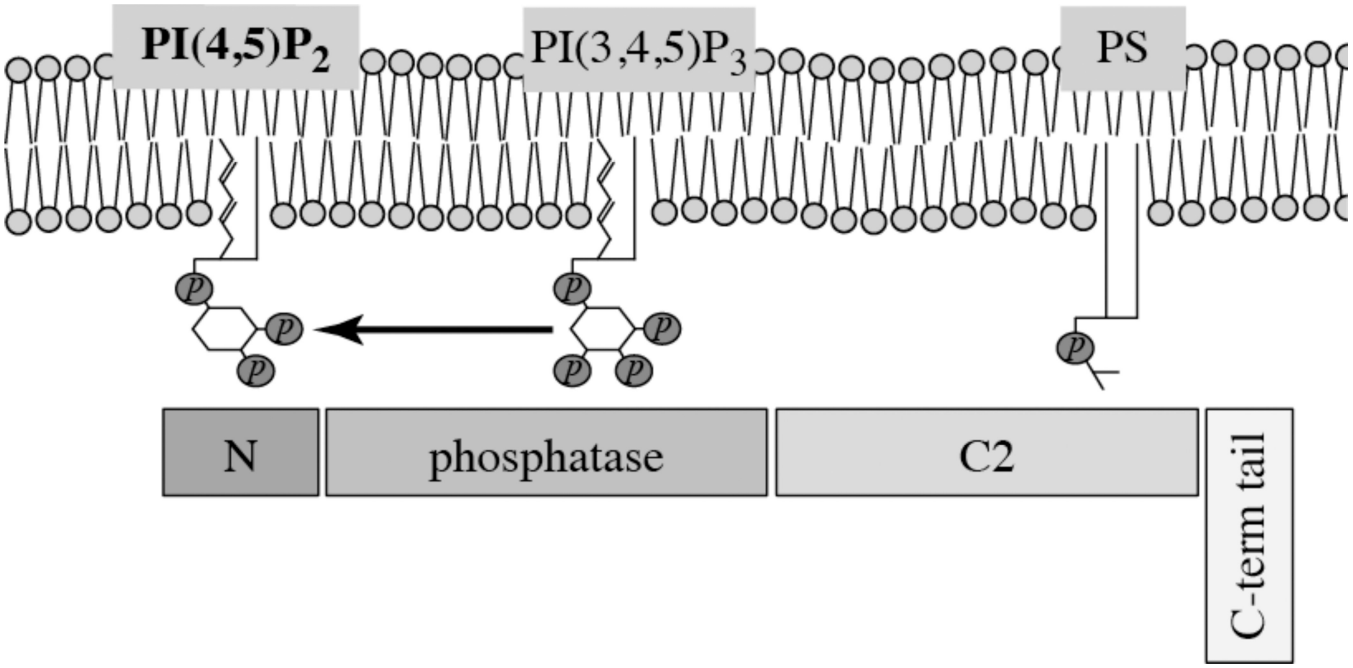

Figure 2.
PTEN binds to multiple anionic lipids in biological membranes. The N-terminus domain binds $PI(4,5)P_2$, whereas the phosphatase domain binds its substrate $PI(3,4,5)P_3$. The C2 domain binds anionic lipids such as PS. The C-terminal tail is presumed to have regulatory functions.

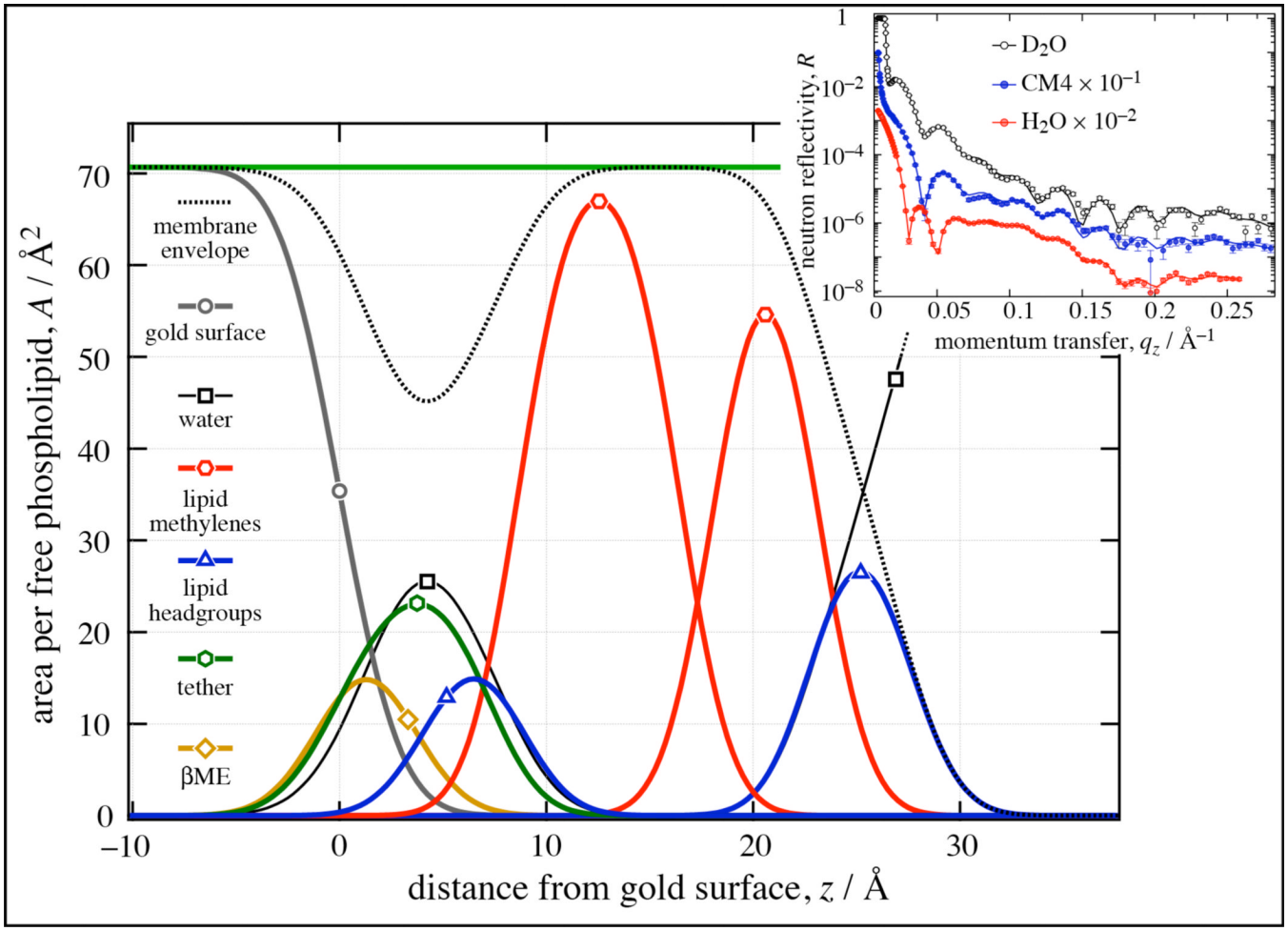

Figure 3.

Exemplary NR data set (proportion of reflected neutrons *vs.* momentum transfer, $\vec{q}_z = \vec{k}_{out} - \vec{k}_{in}$) and its interpretation in terms of the thermally broadened distribution of a molecular fragments across the interface between a gold film on Si and aqueous buffer. Shown is an stBLM with its bilayer composed of (chain-deuterated) DMPC (dimyristoylphosphatidylcholine) [123]. The NR of the stBLM (inset) has been measured in D_2O, H_2O, and a mixture of the two with a neutron SLD (nSLD) of 4×10^{-6} Å^{-2}, termed 'CM4'. A model was then refined by simultaneously fitting three data sets. The resulting decomposed nSLD profile is shown in the main figure. For clarity, distributions of the lipid methyl groups in the bilayer center and the glycerol backbone of the tether lipid, which were also quantified in the model, have been omitted in the plot. By accounting for the chemical connectivities and volumes of the molecular subfragments shown in the distributions, the parameter space could be greatly deduced, so that the decomposed nSLD profiles can be determined with high confidence.

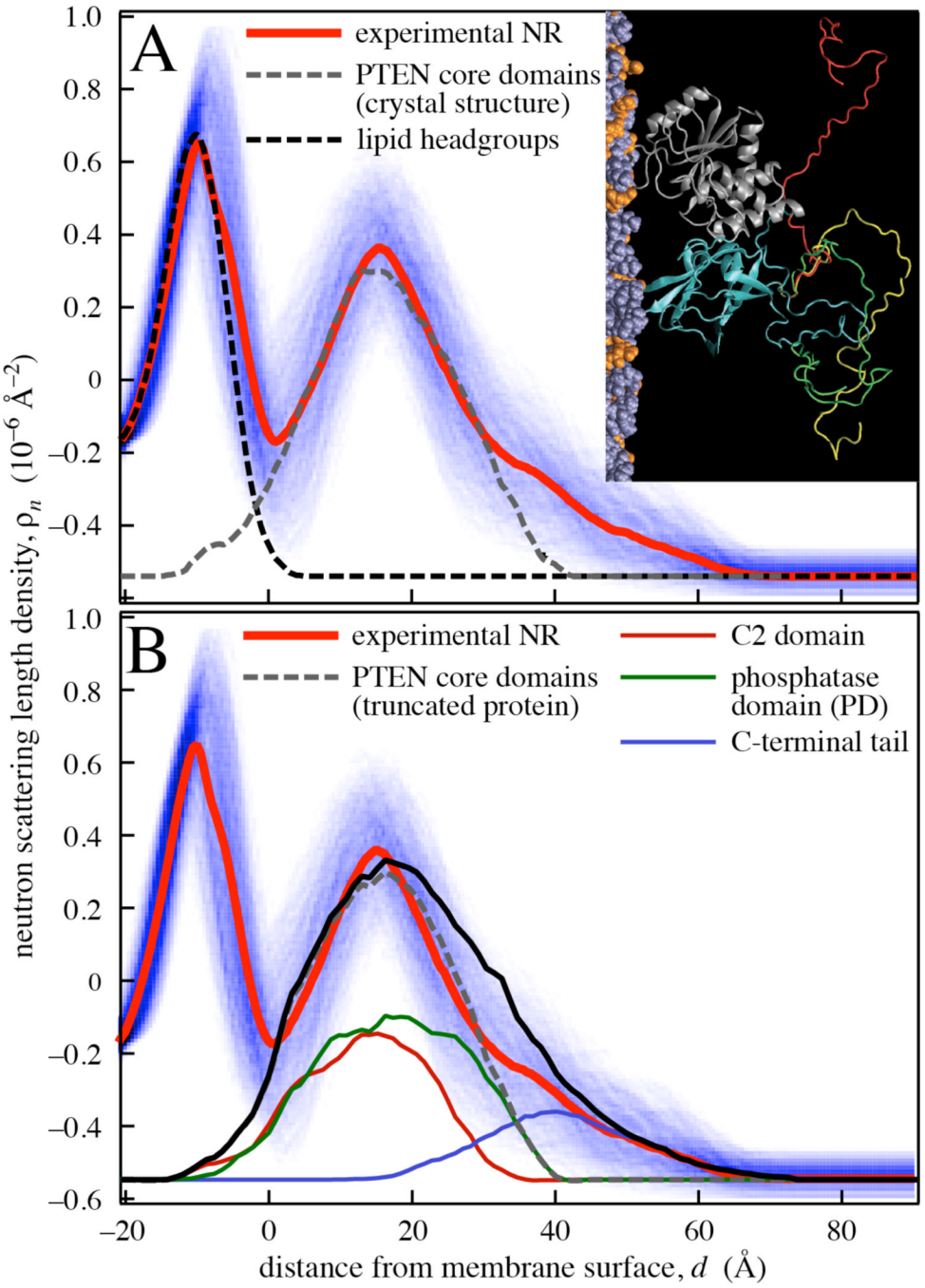

Figure 4.

Neutron scattering length density distribution of a PC/PS stBLM with bound wild-type PTEN from experimental results (red) and its interpretation (A) in terms of placing the crystal structure of a truncated PTEN variant [71] and (B) in terms of all-atom MD simulations (Shenoy et al., submitted). The shaded blue band indicates the confidence intervals around the best-fit model (red line) determine by Monte-Carlo data resampling [114]. The inset in panel A shows a PTEN model based on the crystal structure placed on the bilayer with a few alternate conformations of the C-terminal tail (colored red, yellow, green, and blue) that are consistent with the experimental nSLD profile.

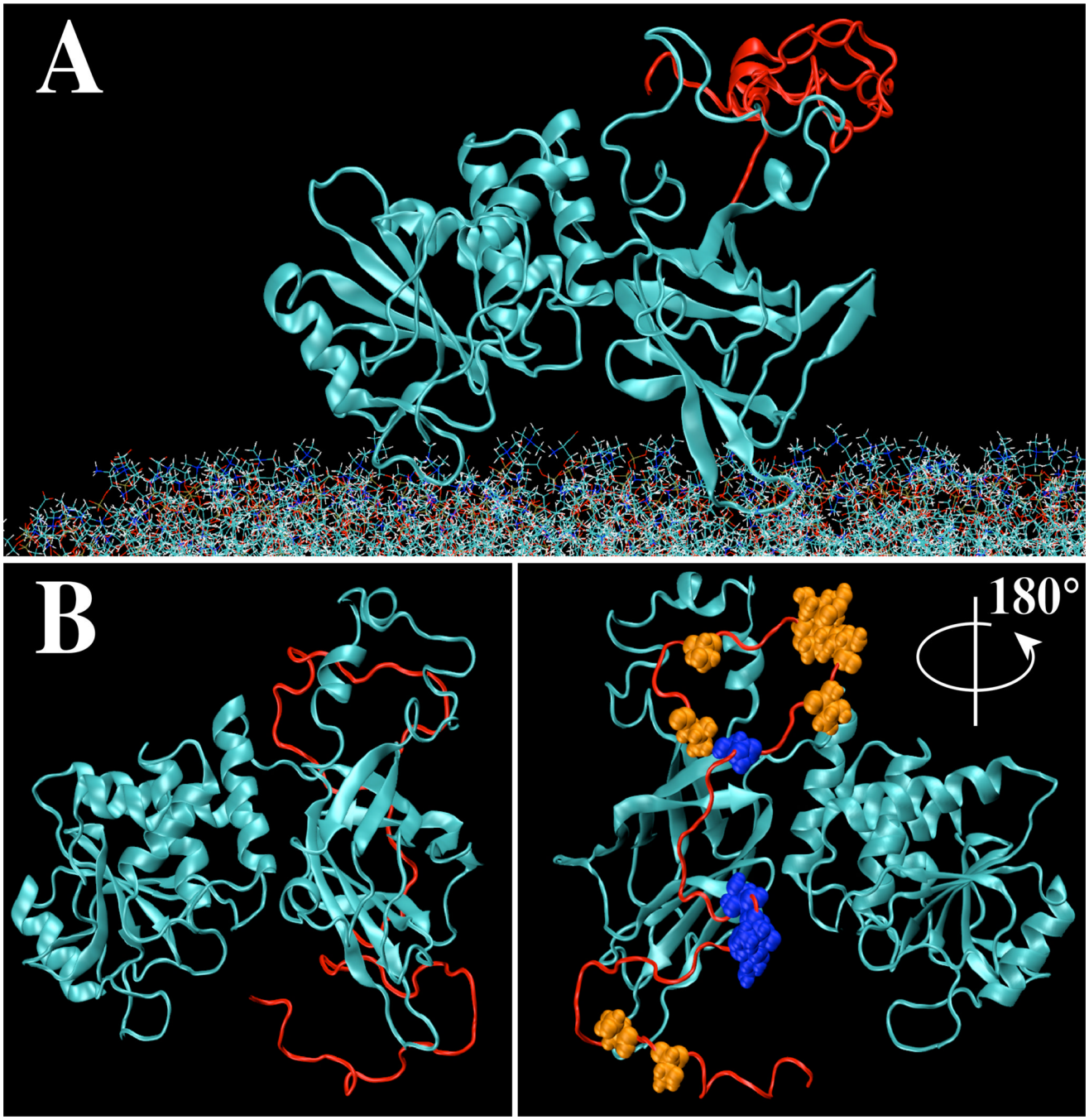

Figure 5.

All-atom MD simulation snapshots of wild-type PTEN on a PC/PS (2:1) membrane (A) and in solution (B). For clarity, water molecules and dissolved ions (100 mM NaCl) are not shown. The general organization of the two core domains, C2 and phosphatase domains, is very similar, but in the membrane-bound structure, the protein is slightly more flattened against the membrane surface. Both core protein structures differ slightly from the crystal structure [45]. The flexible C-terminal tail (red), which is absent in the crystal structure, shows grossly different organization on the membrane-bound and the dissolved protein. On the membrane-bound protein, the net negatively charged tail is electrostatically repelled from the anionic bilayer surface (A). In distinction, it wraps around the C2 domain in

solution and obstructs the membrane-binding interface partially (left in panel B). In the rotated view (right in panel B), Ser and Thr residues are shown in blue and maroon, respectively. Known protein phosphorylation sites such as S370, S380 and S385 are located in exposed positions on the tail and well amenable to phosphorylation. In particular S380 and S385 define a prominent kink in the wrapped tail, which suggests that phosphorylation could lock this conformation in place.